DESIGN AND TEST OF A CLAMPING-SHEAR INTRA-ROW WEEDING DEVICE
/
夹持剪切式株间除草装置设计与试验

Jiacheng ZHOU, Min FU*, Jianhao CHEN, Ji CUI
Northeast Forestry University, College of Mechanical and Electrical Engineering, Harbin / China;
Tel: +86 15663688203; E-mail: fumin1996@163.com
DOI: https://doi.org/10.35633/inmateh-75-04

Keywords: *mechanical weeding, inter-row weeding, weeding device, weeding shovel, ridge planting*

ABSTRACT

Aiming at the complexity and insufficient adaptability of current weeding devices for ridge tillage, this paper presents the design of a clamping-shear weeding device that mimics the hand-grabbing motion. Through the force analysis of the weed root system, the optimal shovel surface inclination angle is determined to be 10°~40°. To ensure the sliding cutting condition, the shovel blade angle is calculated and determined as 30°. Based on the Mohr-Coulomb shear theory, the shovel width is set at 50 mm. A single-factor test was conducted with the soil penetration depth of 40 mm and the clamping-shear speed of 4 cm/s, the results showed that the weed removal rate was over 85% and the crop injury rate was less than 6%. The optimal performance was observed with the shovel inclination angle of 30°.

摘要

针对现有垄作田间株间除草装置结构复杂、适应性差等问题，本文设计了一种模仿人手抓取操作的夹持剪切式除草装置。通过对杂草根系的受力分析，确定最佳铲面倾角为10°~40°。以满足滑切条件为原则，对铲刃倾角进行分析计算，确定铲刃角为 30°。基于摩尔-库仑剪切理论，确定除草铲宽度为 50mm。设定入土深度40mm、夹持剪切速度4cm/s，进行了铲面倾角单因素试验，结果表明：除草率在85%以上，伤苗率在6%以下，当铲面倾角为30°时，除草性能为最优值。

INTRODUCTION

Ridge tillage is one of the important farming methods in China, cultivating numerous food crops and supporting significant benefits to society, ecology, and economy (*Liang et al., 2022*). However, weeds grow disorderly on the ridges and compete with crops for sunlight, water, and nutrients, resulting in a decrease in crop yield and quality, causing huge losses to the agricultural economy (*Li et al., 2022; Ahmad et al., 2020*). To reduce labor costs and minimize environmental pollution, mechanical weeding is considered an ideal method (*Fang et al., 2022; Dilipkumar et al., 2020*). According to different weed operating areas in the field, mechanical weeding can be divided into intra-row weeding and inter-row weeding (*Bing et al., 2021*). Since intra-row weeds are closer to crops, there is a higher risk of damaging crops when removing weeds. Therefore, intra-row weeds are more difficult to control than inter-row weeds (*Longzhe et al., 2021*). At present, the optimization and innovation of intra-row weeding devices have become the research and focus of many scholars.

From the perspective of function, intra-row weeding devices can be divided into those that cut weed roots, those that separate weeds from soil, and those that combine both functions. Devices that cut weed roots mainly include rotary discs (*Pérez-Ruiz et al., 2011*) and swing hoes (*Huang et al., 2012*). The rotary discs were used earlier, and the weeding blades reciprocated rotating between crops to achieve the two actions of avoiding crops and weeding. They have a simple structure, but they cannot separate weed roots from the soil, therefore, weed control is not effective. The swing hoes mainly use the reciprocating swing of the weeding blades to achieve the actions of avoiding crop and weeding. The structure of this device is relatively compact and the crop injury rate is low, but current models use the pneumatic system to drive the swing weeding shovel, and the supporting power system is complex and heavy, making it unsuitable for lightweight operations. Devices that cut weed roots offer good crop-avoidance performance and minimize the risk of crop damage. However, the roots remain in the soil, leading to incomplete weeding. Devices that separate weeds mainly include finger weeder (*Riemens et al., 2007*), brush weeder (*Ziwen et al., 2015*), torsion weeder (*Cirujeda et al., 2013*) and cycloid hoe (*Hu et al., 2012*). The first three are relatively common weeding devices, but they can only remove weeds with shallow root systems and have a high risk of damaging crops; the cycloid hoe is

also a commonly used weeding device. Research on the cycloid hoe intra-row weeding device conducted by Hu Lian et al (*Hu et al., 2012*) shows that the weeding effect is remarkable and the damage to crops is less than 8%. However, the cycloid hoe structure is complex, the maintenance cost is high, and the control is difficult. Weeding devices that separate weeds can completely remove weeds from the soil, but there is a certain risk of damaging the crops. The main hybrid weeding devices include the rotary hoe (*Qinsong et al., 2022*). This device uses the rotation of the rotary hoe, and the needle teeth penetrate the soil to cut the weed roots and take them away from the soil. The hybrid type has a better weeding effect. However, the mechanism is generally complex and the production cost is high.

In summary, most existing intra-row weeding devices suffer from complex structures, poor adaptability, high crop injury rates, and suboptimal weeding performance. To address these challenges, this paper designs a clamping and shearing intra-row weeding device tailored for corn ridge fields, particularly for operations during the 3-4 leaf stage. The design mimics the hand-grasping motion, with a parallelogram mechanism used in the finger component to reduce drive elements and simplify the device's structure. The weeding device is mounted on a six-axis robotic arm, leveraging the arm's multi-degree-of-freedom and flexibility to perform crop-avoidance and weeding tasks. This enhances the device's field adaptability and minimizes crop damage. Key parameters are designed, and the device's effectiveness is validated through tests using crop injury and weed removal rates as evaluation indexes.

MATERIALS AND METHODS

Weeding device design

Weeding field environment

Ridge tillage is the most common farming method in China, with ridge parameters varying by region. In plain areas, ridge heights (H) range from 160~350 mm, ridge spacing (D1) from 500~1000 mm, ridge top width (W1) about 300 mm, and ridge bottom width (W2) about 600 mm. Taking 3~5 leaf stage corn field as an example, the intra-row ridge spacing (D2) is about 240~300 mm, with the planting ridge parameters shown in Fig. 1. Weeds grow unorderly on the ridges. While tillage can effectively remove weeds between rows, intra-row weeds must be removed precisely to avoid accidentally damaging crops. According to field surveys and relevant literature (*Fujun et al., 2018*), weed roots typically extend about 20 mm below the surface, while corn roots at the same depth have a radial spread of about 50 mm. To protect crop roots, the diameter of the crop protected area is set to 60 mm.

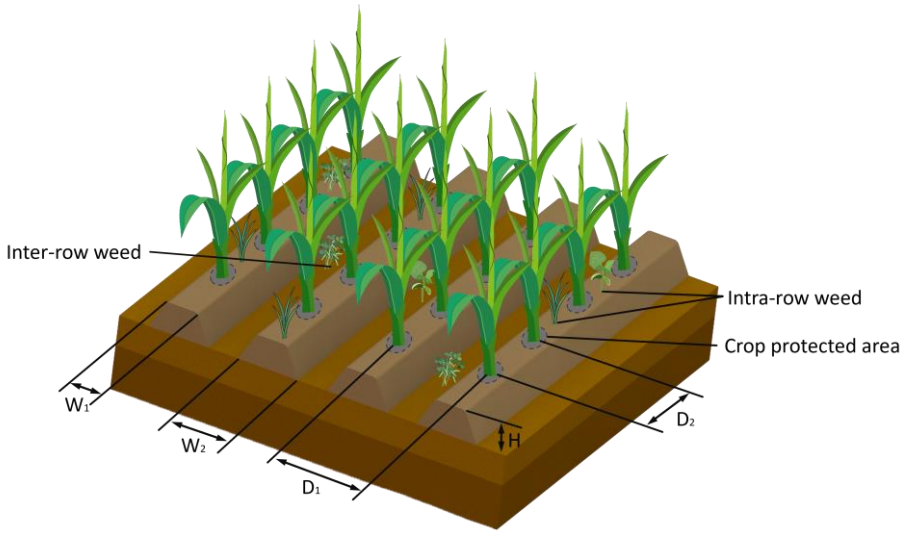

Fig. 1 - Ridge parameters

Weeding device configuration design

A human-like mechanical gripper is highly effective at grasping various objects due to its flexibility and adaptability (*Bircher et al., 2021*). Inspired by this, the weeding device in this paper is designed using the human hand as a bionic prototype. The human hand's structure primarily consists of an open kinematic chain with a series of moving and rotating joints. The configuration of the weeding device is divided into two main parts: the fingers and the palm. The fingers consist mainly of rotating joints, while the palm features moving joints. Key considerations in designing the fingers include the number and structure of the bionic fingers.

Having too many bionic fingers can complicate the structure and make control more difficult. Therefore, the number of bionic fingers should be minimized, provided the weeding function is maintained. For the palm, important factors include the connection between the palm and fingers, as well as the layout of the bionic fingers on the palm.

The configuration of the bionic weeding device designed in this paper is shown in Fig. 2. The device features four fingers, each with two degrees of freedom, comprising two joints and two connecting rods. The joints control the rotation angles of the connecting rods, allowing the fingers to bend by adjusting these angles. The fingers are symmetrically distributed on either side of the palm, which has one degree of freedom. The connection between the fingers and the palm is achieved through a slider pair, enabling the fingers to open and close.

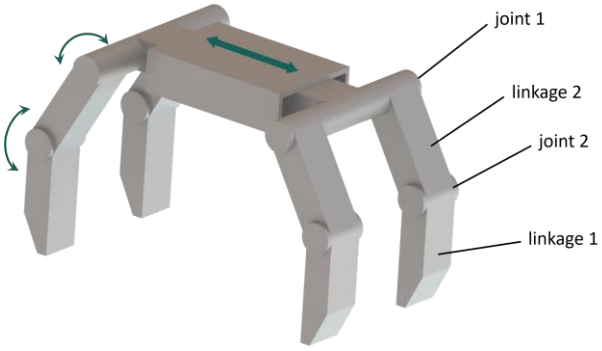

Fig. 2 - Weeding device configuration diagram

Weeding device structure design

Based on the configuration design described in the section 2.2, each finger has two degrees of freedom. To achieve full constraint, two drive elements are necessary. However, directly adding a drive element to the second joint would result in a bulky finger structure and require a large driving torque. To address this, a multi-link mechanism is employed for the single-finger design. By utilizing the characteristics of a parallelogram mechanism, a revolute pair is added to introduce a constraint, allowing the avoidance of placing drive elements at the second joint. This design makes the mechanism compact and lightweight. To further simplify the structure, the two fingers on the same side are driven synchronously by a double-head servo. The distal end of the finger, designed for weeding, is shaped like a cross-finger to closely mimic a human hand. The design model of the finger mechanism is shown in Fig. 3.

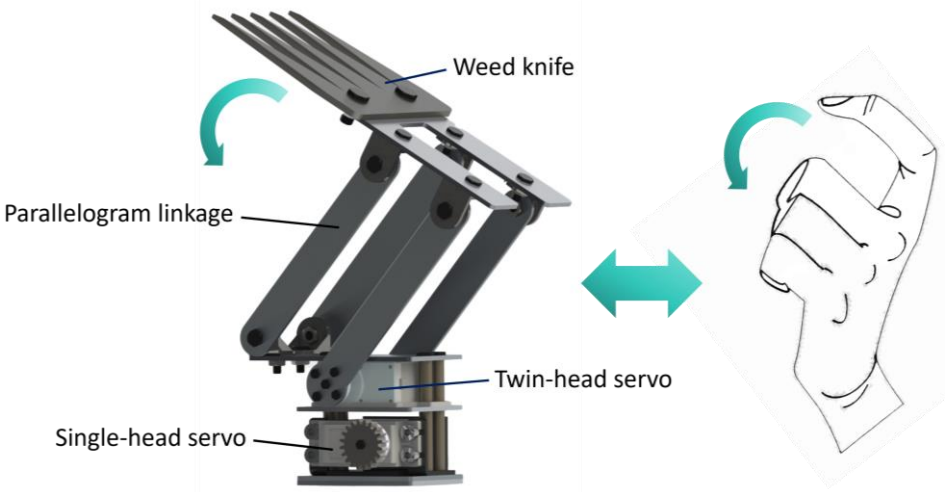

Fig. 3 - Finger design model

The design model of the palm is shown in Fig. 4. A single-head servo serves as the power source, driving the fingers at both ends of the palm. The inward and outward opening and closing movements of the fingers are achieved through a gear rack transmission mechanism.

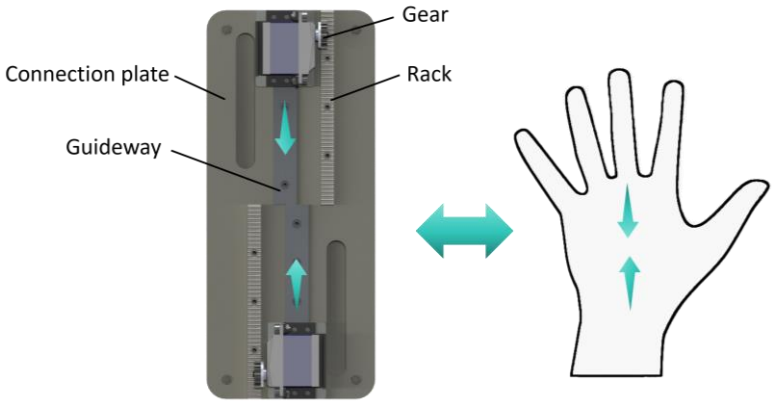

Fig. 4 - Palm design model

The overall structure of the weeding device is shown in Fig. 5. A double-head servo is connected to the second connecting rod of the two fingers on the same side, providing the necessary driving torque. This second connecting rod acts as a power arm, transmitting force to the weeding shovel via a parallelogram mechanism, allowing the shovels on both sides to mesh inward. The fingers on the same side are mounted on a shared slider, with a single-head servo driving their opening and closing along a guide rail through a gear rack transmission, thereby enabling the claw's movement.

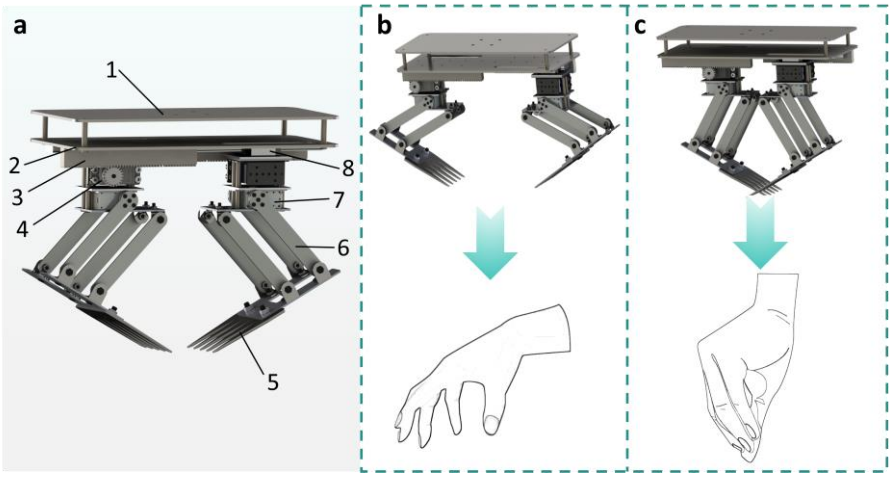

Fig. 5 - Overall structure of weeding device

(a). 3D diagram; (b). open state; (c). closed state

1.fixed plate; 2.connecting plate; 3.rack; 4.single-head servo; 5.weeding shovel; 6.connecting rod; 7.double-head servo; 8.slider

The principle of avoiding crop and weeding of the weeding device

The weeding device is mounted on a six-axis robotic arm, and the operation process is divided into the avoiding crop process and the weeding process. The weeding operation is shown in Fig. 6.

(a)When the operation begins, the visual system first detects crops and weeds. If no weeds are detected, the robotic arm positions the weeding components in the neutral position between the rows. When the visual system detects weeds, a crop protection and a weeding areas are constructed.

(b) After identifying and locating the weeds, the robotic arm, receiving signals from the control system, maneuvers the weeding device to bypass the crops and position itself over the weeding area at an appropriate height, avoiding the crops.

(c) The weeding device’s two double-head servos rotate the second connecting rod, causing the weeding shovels to move toward the center. The tips of the shovels penetrate and break the soil surface, initiating the weeding process.

(d) Once the soil-breaking is completed, the double-head servos cease rotation. Then, the single-head servos engage, rotating gears on a rack that slides the two clamping claws toward the center along the guide rail. The weeding shovels advance into the field ridge at a fixed angle, continuing to break the soil. The root-soil complex is then sheared under the combined effects of gravity and soil friction, gradually lifting along the shovel surface as the shovels mesh, initially separating the weed roots from the soil. Once the shovels completely mesh and shear the weed roots, the single-head servos stop.

(e) Finally, the robotic arm lifts the weeding device, completely separating the weeds from the soil. After the weeds are clamped and removed from the soil, all servos reverse direction, returning the weeding device to its initial state, simultaneously releasing the weeds, thereby completing the weeding operation.

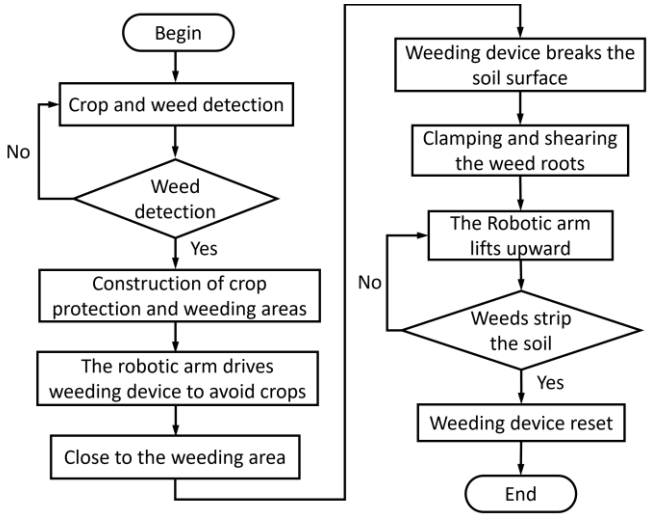

Fig. 6 - Flow chart for the weeding operation

Design of key parameters of weeding device

In order to meet the operation requirements of the weeding device, its key parameters are designed in this paper. These requirements include minimizing soil excavation during weed removal, possessing the ability to crush clay, incorporating a self-cleaning function in the weeding shovel to prevent grass and soil buildup, and ensuring excellent wear resistance.

Shovel surface inclination angle

The integrity of weeds is closely linked to the stability of their roots. Therefore, to ensure the complete removal of weeds from the soil, it is essential to disrupt the stability of the weed roots. The force analysis during the clamping and shearing process is shown in Fig. 7.

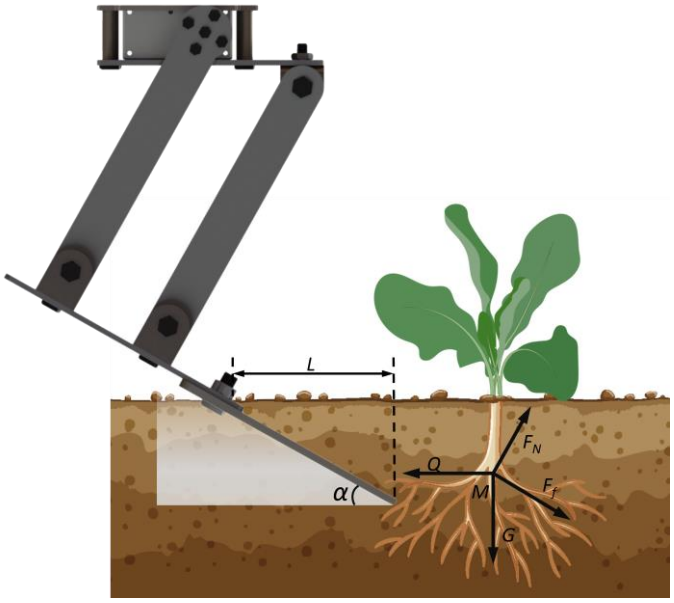

Fig. 7 - Force analysis diagram of weed root

Note: F_N is the support of weeding shovel to weed roots; F_f is the friction between root-soil complex and weeding shovel; G is the gravity of weed roots; Q is the force required to move the weed; α is shovel surface inclination angle; point M is the center of the weed roots; L is the projection length of weeding shovel in the horizontal direction

From the force analysis in Fig. 7, the force on the weed root in the X and Y directions is:

$$F_f \cos\alpha + F_N \cos\left(\pi/2-\alpha\right) = m_0 a_x \quad (1)$$

$$F_N \sin\left(\pi/2-\alpha\right) - F_f \sin\alpha - G = m_0 a_y \quad (2)$$

This is obtained from the momentum theorem:

$$\left[F_f \cos\alpha + F_N \cos\left(\pi/2-\alpha\right)\right]\Delta t = m_0 v \quad (3)$$

where:

m_0 is the quality of weeds, kg; Δt is the time of weeding shovel acting on weeds, s; v is inward clamping-speed of weeding shovel, cm/s; a_x is acceleration of weed root moving in horizontal direction, cm/s^2; a_y is acceleration of weed root moving in vertical direction, cm/s^2.

From Eq. (1) and (2), it is evident that a_x increases with an increase in the shovel surface inclination angle, while a_y decreases as the angle rises. Eq. (3) shows that when the clamping speed v of the weeding shovel is constant, an increase in the shovel surface inclination angle leads to a decrease in the L. This results in a shorter horizontal contact time between the weeds and the weeding shovel, increasing the impulse. Consequently, as the shovel surface inclination angle rises, the stability of the weed root system diminishes, making it easier to disrupt the roots. However, if the angle is excessively large, the resistance encountered during the clamping shear of the weeding shovel will also increase. Combined with the analysis of the operation process of the weeding shovel and the root-soil complex, the mechanical relationship between the two is obtained:

$$F_f + G\sin\alpha = Q\cos\alpha \quad (4)$$

$$G\sin\alpha + Q\sin\alpha = F_N \quad (5)$$

$$F_f = \mu_1 F_N \quad (6)$$

$$\alpha \le \operatorname{arctg}\frac{Q-\mu_1 G}{\mu_1 Q+G} \quad (7)$$

where: μ_1 is the friction factor between soil and weeding shovel.

Through preliminary field tests, it was found that the force required to move the weeds was 10 N, the weight of the weed roots was 0.05 N, and the friction factor between the soil and the weeding shovel was 0.7. Applying these values to Eq. (7), it was determined that α ≤54°. However, when α ≤10°, the depth of the weeding shovel's penetration into the soil is insufficient, preventing complete weed removal. Based on this analysis and referencing relevant literature (*Jinchuan et al., 2017*), the optimal range for the weeding shovel inclination angle is 10°≤ α ≤40° to ensure effective weeding while minimizing working resistance.

Shovel blade angle

During the weeding process, the weeding shovel must demonstrate effective soil penetration and a self-cleaning function for its surface. To achieve this, it is essential to ensure that the sliding cutting force of the soil on the blade exceeds the friction force between the soil and the blade. The force of the weeding shovel blade designed in this paper is shown in Fig. 8.

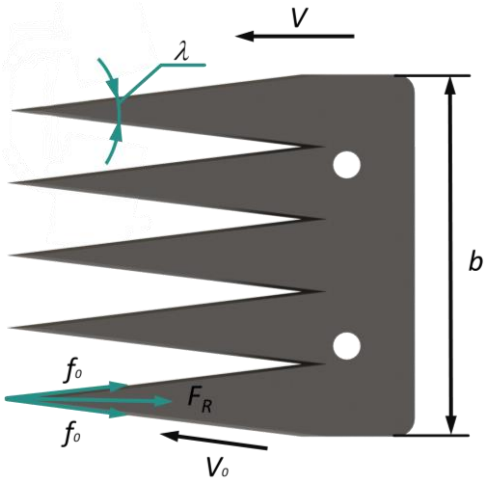

Fig. 8 - Force analysis diagram of weeding shovel blade

Note: F_R is the sliding cutting force on the blade, N ; f_0 is the friction between soil and shovel blade, N; v_0 is the sliding cutting speed, cm/s.

Sliding cutting conditions should meet:

$$F_R \sin(90^\circ - \frac{\lambda}{2}) \geq f_0 \tag{8}$$

$$f_0 = \tan\varphi F_R \cos(90^\circ - \frac{\lambda}{2}) \tag{9}$$

where:

λ is shovel blade angle, (°); φ is the friction angle between soil and weeding shovel surface, (°).

From Eq. (8) and Eq. (9), shovel blade angle λ should be satisfied:

$$90^\circ - \frac{\lambda}{2} \geq \varphi \tag{10}$$

$$\mu_2 = \tan\varphi \tag{11}$$

where:

μ_2 is the friction factor between weed root and weeding shovel.

It can also be seen from Fig. 8 that the relationship between v and v_0 is :

$$v_0 = v\cos\frac{\lambda}{2} \tag{12}$$

Through the actual field measurements and reference to relevant literature (*Jinchuan et al., 2017*), the friction factor between the soil and the weeding shovel is 0.569~0.718, and the friction factor between the weed root and the weeding shovel is 0.89~0.97, so it is enough to meet the friction factor between the weed root and the weeding shovel, and it can be brought into the Eqs. (10) and (11) to calculate that $\lambda \leq 120°$ can meet the requirements. It can be seen from Eq. (12), that the smaller the λ , the smaller the v_0, so the weeding shovel weeding process is more stable, however, when $\lambda < 30°$, the weeding shovel strength is greatly reduced, resulting in weeding shovel wear and tear aggravated, and easy to cause the shovel surface bending, so the weeding shovel blade angle is designed for 30°.

Weeding shovel width

In order to further improve the performance of the weeding device, reduce the resistance in the weeding process, and ensure the smooth shear removal of the weed root-soil complex, the weeding shovel width is designed. In order to completely remove the weed root, the weeding shovel width should be greater than the radiation diameter of the weed root. The weeding shovel width is calculated as:

$$w \geq d + \varepsilon + n \tag{13}$$

where:

w is the weeding shovel width, mm; d is the radiation diameter of weed roots, mm; n is the weeding shovel operation deviation; ε is the standard deviation of weed root diameter.

Through relevant literatures and field research (*Longzhe et al., 2021*), the depth of weed roots under the surface is about 20 mm, the radiation diameter is about 40 mm, the weeding shovel operation deviation is 7 mm, and the standard deviation of weed root diameter is 3 mm. Therefore, the width of weeding shovel should be $w \geq 50$mm.

According to the shovel structure resistance model of Mohr-Coulomb soil shear theory proposed by *Wheeler et al., (1996)*, the resistance during the inward clamping process of the weeding shovel is also related to the weeding shovel width. The resistance model is shown in Fig. 9. When the weeding shovel is clamped and sheared inward at speed v, the soil in the triangular ABC area in front of the weeding shovel produces resistance P to the shovel surface, which can be divided into horizontal force F_x and vertical force F_y. In the absence of other external forces applied to the soil:

$$F_x = \left(\gamma h^2 N_\gamma + chN_{ca}\right)[w + h(m - (m-1)/3) + \gamma v^2 N_a h(w + 0.6h)]\sin(\alpha + \varphi) \tag{14}$$

$$F_y = \left(\gamma h^2 N_\gamma + chN_{ca}\right)[w + h(m - (m-1)/3) + \gamma v^2 N_a h(w + 0.6h)]\cos(\alpha + \varphi) \tag{15}$$

where:

γ is the soil volume weight, kg·m^{-3}; c is the soil cohesion, kN·m^{-2}; h is the depth of weeding shovel into soil, mm; m is the soil fracture width-depth ratio; N_γ is the soil gravity coefficient; N_{ca} is the soil bonding coefficient; N_a is the soil inertia coefficient.

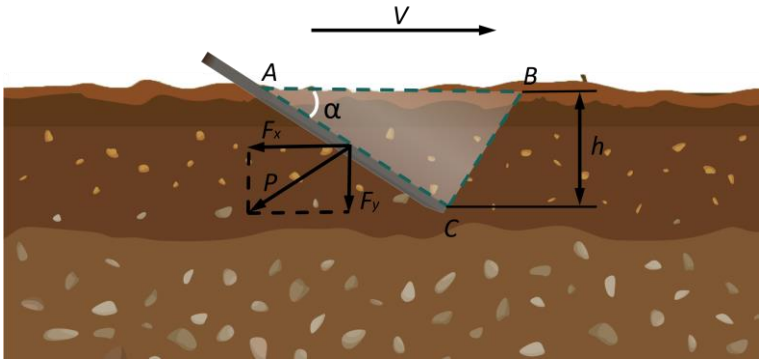

Fig. 9 - Resistance model diagram

Therefore, the resistance P is:

$$P = \left(\gamma h^2 N_\gamma + chN_{ca} + \gamma v^2 hN_a\right) w \tag{16}$$

It can be seen from Eq. (16) that under the condition of a certain clamping speed, the resistance of the weeding shovel is linearly related to the width of the shovel surface, and the larger the width of the shovel surface, the greater the resistance of the weeding shovel. Therefore, in the case of smooth shearing and removing weeds, the weeding shovel width should be as small as possible. Combined with Eq. (13), the weeding shovel width is designed to be 50 mm, which can ensure that the weeding shovel can completely remove the weeds under the condition of small resistance.

Test and result analysis

Test condition

This test simulated the corn ridge field environment and was conducted in the Robotics Laboratory of the School of Mechanical and Electrical Engineering, Northeast Forestry University. The main test equipment includes a weeding device, AUBO-E5 robotic arm, LegionY7000P computer, mobile power supply, etc., as shown in Fig. 10. The weeding device is installed on the AUBO-E5 robotic arm test platform, and the speed of the robotic arm is adjustable.

The constructed ridge length is 3 m, the ridge distance is 600 mm, the average ridge height is 200 mm, and the soil water content is 17%~18%. The focus of this study is to verify the weeding effect of the weeding device. Therefore, in this test, the 3-4 leaf stage corps with similar sizes were used to replace the real corns and the weeds were transplanted to the weeds growing in the natural environment of the field. In order to reduce the test error, the distribution of crops and weeds in each group was as consistent as possible. The sample crop distance is 240~300 mm, and the weed density is 0.01~0.02 plants/cm^2.

Fig. 10 - Test environment

1. weeding device; 2. robotic arm; 3. desktop computer; 4. control panel; 5. mobile power supply

Test method

Based on the determination of key parameters for the weeding components, insights from relevant literature, and field testing experience, it is evident that a small shovel surface inclination angle negatively impacts the weeding effect, while a large inclination angle increases weeding resistance. Therefore, the selected inclination angle is set to 10°~40°, and a single-factor test is conducted. The weeding operation process is illustrated in Fig. 11.

The weeding device remains in an initial state, ready for operation. The visual system identifies and locates the weeds, after which the robotic arm drives the weeding device to avoid the crops and position itself in the designated weeding area. The weeding device, powered by two sets of steering engines, performs the actions of breaking the soil and clamping and shearing the weeds roots. Once complete, the mechanical arm lifts the weeding device to separate the weeds from the soil. After the weeding operation, the mechanical arm resets the device in preparation for the next task.

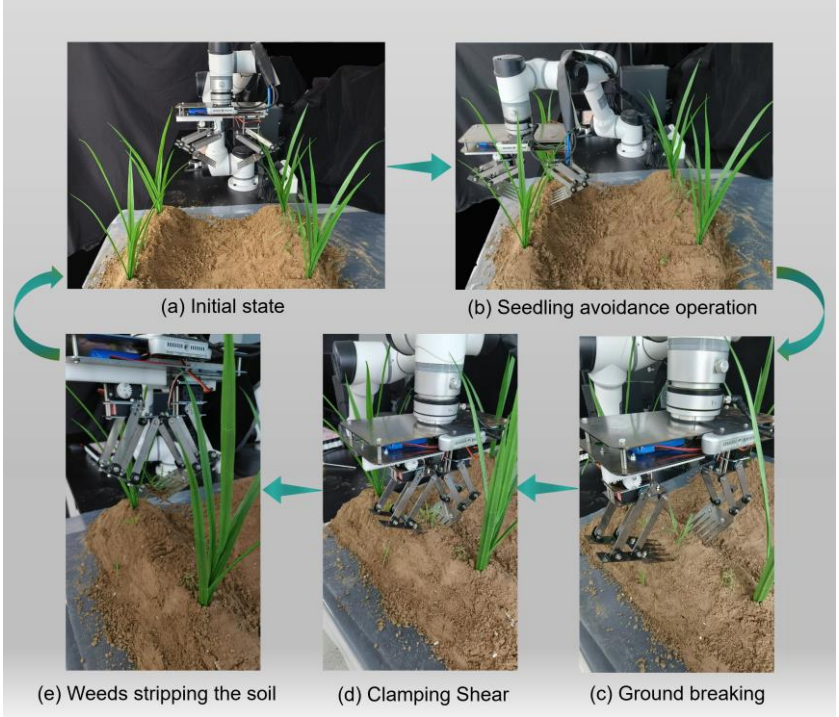

Fig. 11 - Weeding operation process

Weeding operation process

In this test, the crop injury rate and weed removal rate were used as test indexes. Successful weeding was defined by the cutting and destruction of the weeding area and the removal of soil. Due to test limitations, the corns used were at the 3-5 leaf stage. During the test, any sample crops that were uprooted or significantly displaced were considered injured. The number of injuries was counted manually. The calculation formula for the test metrics is as follows (*Bao et al., 2020*):

$$k = \frac{Q_z - H_z}{Q_z} \times 100\% \tag{17}$$

$$s = \frac{M_s}{M_z} \times 100\% \tag{18}$$

where:

k is weed removal rate, %; Q_z is the number of weeds before weeding in the test area; H_z is the number of weed plants after weeding in the test area; s is crop injury rate, %; M_s is the number of injured crops after weeding in test area; M_z is the number of injured crops before weeding in test area.

RESULTS

According to the previous test research, the deepest penetration depth p=40 mm and the clamping shear speed *v*=4 cm/s were set. According to the shovel surface inclination angle ranging from 10° to 40°, the

test was set to 7 levels of 10°, 15°, 20°, 25°, 30°, 35° and 40°. The test results are shown in Table 1, and the relationship between each performance evaluation index and the shovel surface inclination angle is shown in Figure 12.

As shown in Table 1, the weed removal rate exceeds 85%, while the crop injury rate remains below 6%. These results indicate that the weeding device has a reasonable structure and effectively meets the current needs for intra-row weeding in the field.

Table 1

Results of weeding test

Test number	Shovel surface inclination angle (°)	Penetration depth (mm)	Clamping-shear speed (cm/s)	Weed removal rate (%)	Crop injury rate (%)
1	10	40	4	85	3
2	15	40	4	85.5	3.3
3	20	40	4	86.3	3.5
4	25	40	4	87.2	3.7
5	30	40	4	88.8	4.2
6	35	40	4	89.6	4.7
7	40	40	4	90	5.5

As shown in Fig. 13, with the increase of the shovel surface inclination angle, the weed removal rate first increased slowly, and then tended to be stable, and the crop injury rate first increased slowly and then increased sharply. When ≥30°, the weed removal rate tends to be stable, but the crop injury rate rises sharply. Therefore, the suitable range of the inclination angle is 10°~30°. Considering the weeding shovel penetration ability, weeding resistance and intra-row soiling effect in the process of intra-row weeding device, =30° is the better value.

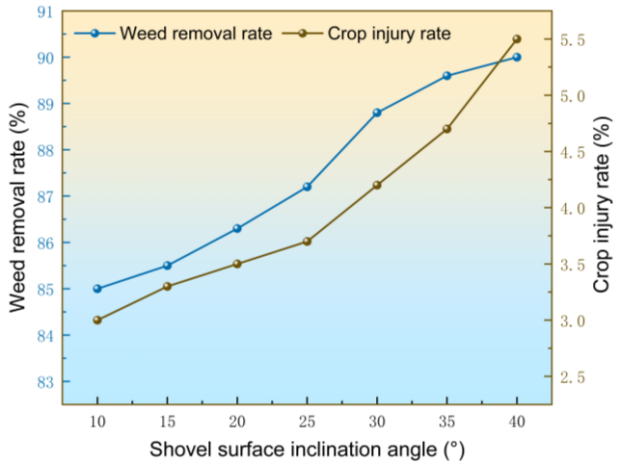

Fig. 12 - The relationship between evaluation index and the shovel surface inclination angle

CONCLUSIONS

(1) For intra-row weeding in ridge fields, a clamping-shear intra-row weeding device was designed by imitating the clamping operation of human hands. The weeding shovel part of the device adopts a parallelogram mechanism, which makes the finger mechanism compact and lightweight, effectively reduces the driving torque, and prolongs the life of the steering gear. The weeding part is mounted on the six-axis manipulator. When the visual system does not recognize the weed, the manipulator drives the weeding part to be in the neutral position between the rows. When the visual system recognizes the weed, the manipulator drives the weeding part to bypass the crop, and the weeding device is accurately moved to the weeding area for weeding.

(2) Through the analysis of the forces acting on the weeding shovel during the clamping and shearing of weeds, it was concluded that the stability of the weed root system decreases as the digging angle of the shovel increases. Consequently, the optimal inclination angle for the weeding shovel was determined to be between 10° and 40°. By analyzing and calculating the shovel blade angle, it is determined that when the blade angle is 30°, there will be no winding grass and soil in the weeding operation. Additionally, a resistance model was established based on the Mohr-Coulomb soil shear theory, leading to the determination of the weeding shovel width, which was set at 50 mm to ensure minimal resistance while completely removing weeds.

(3) On the test platform built in the laboratory, the designed weeding device was tested with the shovel inclination angle as a single factor. The test results showed that the weed removal rate of the weeding device was above 85 %, and the crop injury rate was below 6 %. Meet the requirements of intra-row weeding in the ridge field, and when the shovel inclination angle is 30°, the weeding performance of the device is optimal. The research in this paper can provide a reference for the design and improvement of intra-row weeding devices in ridge fields.

ACKNOWLEDGEMENT

This research is funded by the National Science Foundation of China (Grant No. 51975114).

REFERENCES

[1] Ahmad, F., Qiu, B., Dong, X., Ma, J., Huang, X., Ahmed, S., & Chandio, F. A. (2020). Effect of operational parameters of UAV sprayer on spray deposition pattern in target and off-target zones during outer field weed control application. *Computers and Electronics in Agriculture*, *172*, 105350.

[2] Bao, H. A. N., Chang, G. U. O., Yingling, G. A. O., Qiao, L. I. U., Shuo, S. U. N., & Xiaowei, D. O. N. G. (2020). Design and Experiment of Soybean Intra-row Weeding Monomer Mechanism and Key Components. *Nongye Jixie Xuebao/Transactions of the Chinese Society of Agricultural Machinery*, *51*(6), 112-121.

[3] Bircher, W. G., Morgan, A. S., & Dollar, A. M. (2021). Complex manipulation with a simple robotic hand through contact breaking and caging. *Science Robotics*, *6*(54), 2666.

[4] Bing, X., Decong, Z., Jiaxin, W., & Youzhi, Y. (2021). Workspace analysis of a flame intra-row weeding robot in vegetable field and numerical simulation of propane combustion. *INMATEH-Agricultural Engineering*, *65*(3), 73-81. DPI: https://doi.org/10.35633/inmateh-65-08

[5] Cirujeda, A., Aibar, J., Moreno, M. M., & Zaragoza, C. (2015). Effective mechanical weed control in processing tomato: Seven years of results. *Renewable Agriculture and Food Systems*, *30*(3), 223-232.

[6] Dilipkumar, M., Chuah, T. S., Goh, S. S., & Sahid, I. (2020). Weed management issues, challenges, and opportunities in Malaysia. *Crop Protection*, 134, 104347.

[7] Fang, H., Niu, M., Xue, X., & Ji, C. (2022). Effects of mechanical-chemical synergistic weeding on weed control in maize field. *Trans. CSAE*, *38*(6), 44-51.

[8] Fujun, Z. H. O. U., Wenming, W. A. N. G., Xiaoli, L. I., & Zunfeng, T. A. N. G. (2018). Design and experiment of cam rocker swing intra-row weeding device for maize. *Nongye Jixie Xuebao/Transactions of the Chinese Society of Agricultural Machinery*, *49*(1), 77-85.

[9] Huang, X. L., Liu, W. D., Zhang, C. L., Zhang, Y., & Li, W. (2012). Optimal design of rotating disc for intra-row weeding robot. *Transaction of the Chinese Society for Agricultural Machinery*, 43(6), 42-46.

[10] Hu, L., Luo, X., Yan, Y. A., Chen, X., Zen, S., & Zhang, L. (2012). Development and experiment of intra-row mechanical weeding device based on trochoid motion of claw tooth. *Transactions of the Chinese Society of Agricultural Engineering*, *28*(14), 10-16.

[11] Jinchuan, L., Yimin, Z., Xin, S., Song, M., & Xinpeng, S. (2017). Optimization of the angle of artichoke harvester's second-order flat shovel based on Mathematica. *Ganhan Diqu Nongye Yanjiu*, *35*(2), 282-288.

[12] Liang, Y. G., Hu, W. B., Liu, Y., Li, Y. Y., & Fang, B. H. (2022). The research progress of ridge cultivation mode in China. *Chinese Journal of Ecology*, 41(7), 1414-1422.

[13] Li, Y., Guo, Z., Shuang, F., Zhang, M., & Li, X. (2022). Key technologies of machine vision for weeding robots: A review and benchmark. *Computers and Electronics in Agriculture*, *196*, 106880.

[14] Longzhe, Quan N., Jingyu, Zhang, Wei, Jiang, Hengda, Li, Chunjie, Yang, & Xilin, Zhang. (2021). Development and Experiment of Intra-row Weeding Robot System Based on Protection of Maize Root System. *Nongye Jixie Xuebao/Transactions of the Chinese Society of Agricultural Machinery*, *52*(12), 115-123.

[15] Pérez-Ruiz, M., Slaughter, D. C., Gliever, C. J., & Upadhyaya, S. K. (2012). Automatic GPS-based intra-row weed knife control system for transplanted row crops. *Computers and Electronics in Agriculture*, 80, 41-49.

[16] Qinsong, X., Suming, D., Xinyu, X., Longfei, C., Feixiang, L., & Yinghang, L. (2022). Research on the development status of intelligent field weeding robot. *Journal of Chinese Agricultural Mechanization*, *43*(8), 173.

[17] Riemens, M.M., Groeneveld, R.M.W., Lotz, L.A. P., & Kropff, M.J. (2007). Effects of three management strategies on the seedbank, emergence and the need for hand weeding in an organic arable cropping system. *Weed Research*, *47*(5), 442-451.

[18] Wheeler, P.N., & Godwin, R.J. (1996). Soil dynamics of single and multiple tines at speeds up to 20 km/h. *Journal of Agricultural Engineering Research*, *63*(3), 243-249.

[19] Ziwen, C., Nan, L., Zhe, S., Tao, L., Chunlong, Z., & Wei, L. (2015). Optimization and experiment of intra-row brush weeding manipulator based on planetary gear train. *Nongye Jixie Xuebao/Transactions of the Chinese Society of Agricultural Machinery*, *46*(9).